AIMS Materials Science, 12(2): 278–300.
DOI: 10.3934/matersci.2025015
Received: 25 November 2024
Revised: 18 March 2025
Accepted: 26 March 2025
Published: 07 April 2025

http://www.aimspress.com/journal/Materials

Research article

Optimization of synthesis of cellulose/gum Arabic/Ag bionanocomposite for antibacterial applications

Mohsen Safaei[1,2], Mohammad Salmani Mobarakeh[2], Bahram Azizi[3], Ehsan Shoohanizad[3], Ling Shing Wong[4] and Nafiseh Nikkerdar[5,*]

[1] Division of Dental Biomaterials, School of Dentistry, Kermanshah University of Medical Sciences, Kermanshah 54658, Iran
[2] Advanced Dental Sciences and Technology Research Center, School of Dentistry, Kermanshah University of Medical Sciences, Kermanshah 38647, Iran
[3] Department of Oral and Maxillofacial Surgery, School of Dentistry, Kermanshah University of Medical Sciences, Kermanshah 54658, Iran
[4] Faculty of Health and Life Sciences, INTI International University, Nilai 71800, Malaysia
[5] Department of Oral and Maxillofacial Radiology, School of Dentistry, Kermanshah University of Medical Sciences, Kermanshah 54658, Iran

* **Correspondence:** Email: nikkerdarnafiseh@gmail.com; Tel: +98-933-863-1142.

Abstract: The increasing resistance of microorganisms to conventional antimicrobial compounds requires the development of innovative solutions, such as antimicrobial nanoparticles, to combat antibiotic-resistant infections. This study aimed to optimize the synthesis of a cellulose/gum Arabic/silver (cellulose/GA/Ag) bionanocomposite and evaluate its antibacterial properties against *S. mutans*, a key contributor to dental caries. Using the Taguchi method, we designed nine experiments with varying levels of cellulose (2, 4, and 6 mg/mL), gum Arabic (1, 2, and 3 mg/mL), and silver nanoparticles (2, 4, and 6 mg/mL). The nanocomposite synthesized under optimal conditions (2 mg/mL cellulose, 3 mg/mL gum Arabic, and 6 mg/mL silver nanoparticles) demonstrated the most potent antibacterial activity, reducing the bacterial survival rate of *S. mutans* to 0 Log10 CFU/mL, indicating complete inhibition. Variance analysis revealed that silver nanoparticles had the most significant impact on bacterial survival (53.22%), followed by gum Arabic (35.55%) and cellulose (8.86%). Characterization techniques confirmed the successful formation of the nanocomposite: FTIR analysis indicated hydrogen bonding between cellulose and silver nanoparticles, while XRD confirmed the crystalline structure of the nanocomposite. SEM and TEM images revealed a uniform distribution of

silver nanoparticles within the cellulose–gum Arabic matrix. TGA-DSC analysis showed enhanced thermal stability, with a significant weight loss at 375 °C, corresponding to the degradation of cellulose and gum Arabic. The results demonstrate that the cellulose/GA/Ag nanocomposite, synthesized under optimal conditions, exhibits exceptional antibacterial properties and stability, making it a promising candidate for antimicrobial applications in medical and dental fields.

Keywords: cellulose; gum Arabic; silver nanoparticles; human health; *Streptococcus mutans*; Taguchi method

Abbreviations: *S. mutans*: *Streptococcus mutans*; FTIR: Fourier-transform infrared spectroscopy; XRD: X-ray diffraction; SEM: Scanning electron microscopy; TEM: Transmission electron microscopy; TGA: Thermogravimetric analysis; DSC: Differential scanning calorimetry

1. Introduction

The incidence of communicable illnesses resulting from harmful bacteria is on the rise. *Streptococcus mutans (S. mutans)* is a variety of harmful bacteria recognized as a crucial participant in the commencement and advancement of dental caries. Because of its ability and high capacity to produce extracellular polysaccharides such as dextran and glucan from sucrose to bind to tooth enamel and produce large amounts of acid, *S. mutans* can create a biofilm on the surface of tooth enamel, playing an important role in plaque formation. It can withstand acidic conditions and is immune to typical antimicrobial substances.

The rising occurrence of antibiotic-resistant bacteria has resulted in a greater need to create potent, novel, harmless, and long-lasting antibacterial treatments. These substances can typically be categorized into organic and inorganic compounds, depending on their chemical makeup. Silver (Ag) and its derivatives are minerals that possess germicidal properties, excellent biocompatibility, and an extensive spectrum of antimicrobial actions against bacteria, fungi, and viruses. Hence, they are one of the most crucial antibacterial agents. The increasing prevalence of antibiotic-resistant bacterial infections has become a major global health challenge, driving the need for innovative antimicrobial solutions. Among the various pathogens, *S. mutans* is a primary causative agent of dental caries due to its ability to form biofilms on tooth surfaces and produce acid from sucrose, leading to enamel demineralization. Traditional antimicrobial agents often face challenges such as microbial resistance, toxicity, and limited efficacy, prompting the exploration of alternative approaches, including nanotechnology-based solutions. Ag nanoparticles have emerged as a promising candidate due to their broad-spectrum antimicrobial activity, biocompatibility, and ability to disrupt bacterial cell membranes and DNA replication. However, the effective delivery and stability of Ag nanoparticles in biomedical applications require suitable biopolymer matrices [1,2].

Numerous nanomaterials are employed in a multitude of fields, including sensing technologies, energy generation, catalysis, biotechnology, medicine, electronics, chemistry, physics, material science, biosensors, and computing. Nanoparticles have also gained considerable interest in the fields of medicine and drug development. Previous investigations documented the effectiveness of metal nanoparticles in preventing cancer and fighting bacterial infections [3–7].

Several research studies indicated that the generation of reactive oxygen species (ROS) triggered by these nanoparticles results in the ruin of mitochondria or the demise of normal cells, and the variance in their magnitude is negligible [8].

The characteristics of nanoparticles are intricately linked to their structure and dimension. When talking about nanomaterials, nanocomposites hold a unique position. The constituents of nanocomposites exhibit superior characteristics as a result of the interplay at the interface of the substrate and the strengthening agent. Nanoparticle composites are the principal kind of materials in this category [9,10].

Throughout the past century, studies have been conducted on polymeric substances, their doped counterparts, and their composites to explore potential applications in diverse areas, particularly in the medical sector. Gaining a deeper understanding of the fundamentals of polymers and their structural variations is essential, as they constitute a significant portion of the materials that shape our modern existence. Certain living organisms are considered a crucial source of organic polymers. In recent years, bio-based materials have gained significant attention for their potential in developing sustainable and biocompatible antimicrobial agents [11].

Bacterially synthesized cellulose (BC) and gum Arabic (GA) are two biopolymers that have been extensively studied for their unique properties and applications. BC is an innate biomaterial that possesses exceptional physicochemical characteristics, remarkable mechanical properties, and remarkable water absorption ability. It possesses nanofiber arrangements, is biocompatible and harmless, and has chemical stability, elevated crystallinity, and a broad surface area. Its versatility has been acknowledged in a multitude of domains, such as biomedicine, osseous transplant, synthetic dermis, biological fabricating, odontology fixtures, and injury bandages. Moreover, hybrids derived from bacterial cellulose and fortified with natural or synthetic substances like copolymers, metallic nanostructures, or metallic oxides endowed with antimicrobial characteristics have been manufactured. Numerous research works have been released concerning the amalgamation of silver nanoparticles with bacterial cellulose. Bacterial cellulose, produced by *Acetobacter xylinum* (*A. xylinum)*, is a natural biomaterial with exceptional physicochemical properties, including high mechanical strength, biocompatibility, and water retention capacity. Its nanofiber structure provides a large surface area, making it an ideal matrix for embedding nanoparticles [12,13].

GA or gum Acacia is a consumable biopolymer derived from the exudates of fully-grown trees of *Acacia senegal*, *Acacia seyal (A. seyal)*, *Acacia karroo (A. karroo)*, *Acacia polyacantha (A. polyacantha)*, and *Acacia sieberiana (A. sieberiana)*. Arabic gum is a heteropolysaccharide that is branched and complex, having a neutral or slightly acidic nature. It occurs as a mixture of calcium, magnesium, and potassium salts of a polysaccharide acid known as Arabic acid. Gum Arabic is widely used in the food and pharmaceutical industries due to its emulsifying, stabilizing, and biocompatible properties. This polymer is harmless, has no scent, and is flavorless. This polymer interacts with water, which allows it to be used for a wide variety of purposes requiring texture control, and its pH falls within a nearly neutral range. gum Arabic's ability to form stable complexes with metal nanoparticles enhances the dispersion and stability of Ag nanoparticles in the nanocomposite [14].

In this study, bacterial cellulose and gum Arabic were chosen over synthetic polymers due to their cost-effectiveness and sustainability. Bacterial cellulose can be produced through microbial fermentation using low-cost agricultural byproducts, making it an economically viable option. Similarly, gum Arabic is abundant and readily available, with a lower environmental impact compared to synthetic stabilizers. In contrast, synthetic polymers often require complex synthesis processes and

may pose environmental and toxicity concerns. Furthermore, the performance of the cellulose/gum Arabic/silver (cellulose/GA/Ag) nanocomposite was compared with other antibacterial materials, such as chitosan-based composites and synthetic polymer matrices. The results demonstrated that the cellulose/GA/Ag nanocomposite exhibited superior antibacterial activity against *S. mutans* while maintaining excellent biocompatibility and cost-effectiveness.

Recent studies have demonstrated the potential of cellulose-based nanocomposites in various biomedical applications, underscored by their versatility and potential in various fields [15–18].

Despite significant progress in the development of cellulose-based nanocomposites, several research gaps remain. First, there is a need for more cost-effective and scalable synthesis methods that can produce nanocomposites with consistent properties. Second, the interaction between cellulose, gum Arabic, and silver nanoparticles needs to be better understood to optimize the nanocomposite's antimicrobial properties. Third, there is limited research on the long-term stability and biocompatibility of these nanocomposites in biomedical applications. This study addresses these gaps by employing the Taguchi method to optimize the synthesis conditions for a cellulose/GA/Ag bionanocomposite, ensuring consistent and reproducible results. To achieve this, the co-precipitation synthesis technique was utilized to generate silver nanoparticles. Furthermore, *Acetobacter xylinum* bacteria were used to synthesize cellulose biopolymers through microbial means. Ultimately, a nanocomposite of silver–cellulose–gum Arabic was produced through a direct or in situ synthesis method.

Additionally, we provide a detailed characterization of the nanocomposite's structural, thermal, and antimicrobial properties, offering insights into the interaction between the components and their impact on performance. The novelties of this work lie in the optimization of synthesis conditions, enhanced antimicrobial properties, comprehensive characterization, and cost-effectiveness and sustainability. The primary objective of this study was to optimize the synthesis conditions for the cellulose/GA/Ag bionanocomposite and evaluate its antibacterial properties against *S. mutans*. The results of this study provide valuable insights into the development of cost-effective and sustainable antimicrobial materials for medical and dental applications.

2. Materials and methods

2.1. Materials

The materials used in this study were obtained from reputable sources to ensure the quality and reliability of the experiments. Bacterial cellulose was synthesized using *Acetobacter xylinum* (PTCC 1734), which was procured from the Persian Type Culture Collection (PTCC), Iran. Gum Arabic (GA) was purchased from Sigma-Aldrich (St. Louis, MO, USA), and silver nitrate ($AgNO_3$) was obtained from Merck (Darmstadt, Germany). Trisodium citrate dihydrate ($C_6H_5Na_3O_7 \cdot 2H_2O$), used as a reducing agent in the synthesis of silver nanoparticles, was also purchased from Merck. All chemicals were of analytical grade and used without further purification.

2.2. Synthesis of cellulose biopolymer

The bacterium *Acetobacter xylinum* (PTCC 1734) was procured from the Scientific and Industrial Research Organization of Iran. Nguyen et al. (2008) delineated a modified technique for the production of bacterial cellulose, which was employed to create microbial cellulose [19]. Briefly,

the Hestrin–Schramm culture medium was used for bacterial cultivation under stable conditions for seven days. Then, the mature cellulose film was retrieved from the top of the growth medium, submerged in 0.5 M sodium hydroxide, and heated to 90 °C for 60 min. The resultant cellulose was rinsed with purified water and dehydrated at 40 °C to obtain a fine powder.

2.3. Ag nanoparticle synthesis

Silver nanoparticles (Ag NPs) were synthesized using a co-precipitation method. A 0.01 M silver nitrate ($AgNO_3$) solution was prepared by dissolving $AgNO_3$ in distilled water. The solution was heated to boiling, and 5 mL of a 1% trisodium citrate solution was added dropwise under continuous stirring. The mixture was stirred until it turned light-yellow, indicating the formation of silver nanoparticles. The solution was then cooled to room temperature and centrifuged at 5000 rpm for 15 min to remove any impurities. The resulting silver nanoparticles were washed with distilled water and stored at 4 °C for further use [20].

2.4. Synthesis of cellulose/gum Arabic/Ag nanocomposites

The Taguchi method was employed to optimize the synthesis conditions for the cellulose/GA/Ag nanocomposite. Nine experiments were designed using Qualitek-4 software, with varying concentrations of cellulose (2, 4, 6 mg/mL), gum Arabic (1, 2, 3 mg/mL), and silver nanoparticles (2, 4, 6 mg/mL) (Table 1). The nanocomposites were synthesized by mixing the appropriate amounts of cellulose, gum Arabic, and silver nanoparticle solutions in separate vessels. The mixtures were stirred for 60 min on a magnetic stirrer and then sonicated for 15 min to ensure homogeneity. The resulting solutions were dried in an oven at 60 °C for 24 h to obtain the nanocomposite powder [21].

Table 1. Taguchi design of experiments to evaluate the effects of cellulose/gum Arabic/Ag synthesized nanocomposites on the survival rate of *Streptococcus mutans*.

Experiments	Cellulose (mg/mL)			Gum Arabic (mg/mL)			Ag(mg/mL)		
	2	4	6	1	2	3	2	4	6
1		2			1			2	
2		2			2			4	
3		2			3			6	
4		4			1			4	
5		4			2			6	
6		4			3			2	
7		6			1			6	
8		6			2			2	
9		6			3			4	

2.5. Antibacterial activity

The antibacterial activity of the synthesized nanocomposites was evaluated against *Streptococcus mutans* (ATCC 35668), which was obtained from the Iranian Biological Resource Center (IBRC). The bacteria were cultured on brain-heart infusion (BHI) agar plates for 24 h at 37 °C. A bacterial

suspension with a turbidity of 0.5 McFarland standard was prepared and used to inoculate 96-well culture plates. The plates were incubated for 72 h at 37 °C to allow biofilm formation. The nanocomposites were then added to the wells, and plates were incubated for an additional 24 h. The viability of the bacteria was assessed using the colony-forming unit (CFU) assay [22,23].

2.6. Characterization

Various characterization techniques were employed to examine the characteristics of the constituents and the composite of silver, gum Arabic, and cellulose. A range of analytical methods was used to attain the desired objective. These included Fourier transform infrared spectroscopy (FTIR), utilizing equipment from Thermo (USA) at ambient temperature, X-ray diffraction (XRD) using a Philips X' Pert (40 kV, 30 mA) (Netherlands), scanning electron microscope field emission (FESEM) with a TESCAN MIRA III model (Czech Republic), Energy-dispersive X-ray spectroscopy (EDS) using a MIRA III model SAMX detector (France), and element distribution map (Map) with SAMX detector from TESCAN MIRA II. Additionally, a transmission electron microscope (TEM) was used (TEM Philips EM208S, Netherlands), and Ultraviolet-visible spectroscopy (UV-Vis) was conducted using a Shimadzu UV-160 A model (Japan). Thermogravimetric analysis/differential scanning calorimetry (TGA-DSC) was carried out using a TA Q600 model.

3. Results and discussion

3.1. FTIR analysis

Figure 1 displays the analysis of the structure of the cellulose biopolymer (a), gum Arabic (b), silver nanoparticles (c), and the produced nanocomposite (d) by scrutinizing their FTIR spectra. The absorption of the O–H group is responsible for the 3345 cm^{-1} band observed in the cellulose spectrum, while the stretching and deformation of the C–H group in the glucose structure are indicated by the bands detected at 2893 and 1370 cm^{-1}. The peak at 1612 cm^{-1} corresponds to the absorption of water and the stretching of the O–H group. The FTIR spectrum at 1420 cm^{-1} corresponds to the symmetric bending vibration of $–CH_2$, which is also known as the band of crystallinity, and its reduction is proportional to the decrease in the level of crystallinity in the specimen. The 1055 cm^{-1} absorption band is a result of the –C–O– cluster of secondary alcohols and ether portions present in the arrangement of cellulose, while the 890 cm^{-1} peak signifies the beta-glycosidic linkage among the glucose moieties that constitute cellulose. This bond denotes the level of shapelessness of the specimens: as their strength rises, so does the level of shapelessness of the specimens [24,25].

In the FTIR spectrum of gum Arabic, the wide absorption band at 3000–3500 cm^{-1} (peak at 3415 cm^{-1}) indicates the existence of hydroxyl groups linked to hydrogen, which matches the absorption band of the amine group in this range. The peaks at 2914 and 1600 cm^{-1} are associated with the distortion movements of CH groups. The primary and most robust oscillation patterns attributed to polysaccharide molecules fall within the range of 1000–1100 cm^{-1}. The detected range at 1200–1400 cm^{-1} is linked to C–O and C–O–C oscillation, distinctive of organic polysaccharides. A peak at 1421 cm^{-1} with comparatively weak peak strength is attributed to C–O bond oscillation. The carboxylate groups linked to the gum Arabic molecule exhibit a distinct peak in the range of 1700–1517 cm^{-1} as a result of C=O stretching and N–H bending. Arabic Gum comprises a small quantity of protein with elevated

molecular weight and a substantial quantity of polysaccharide with diminished molecular weight. It appears that glycoprotein clusters are enveloped by polysaccharide rings [26].

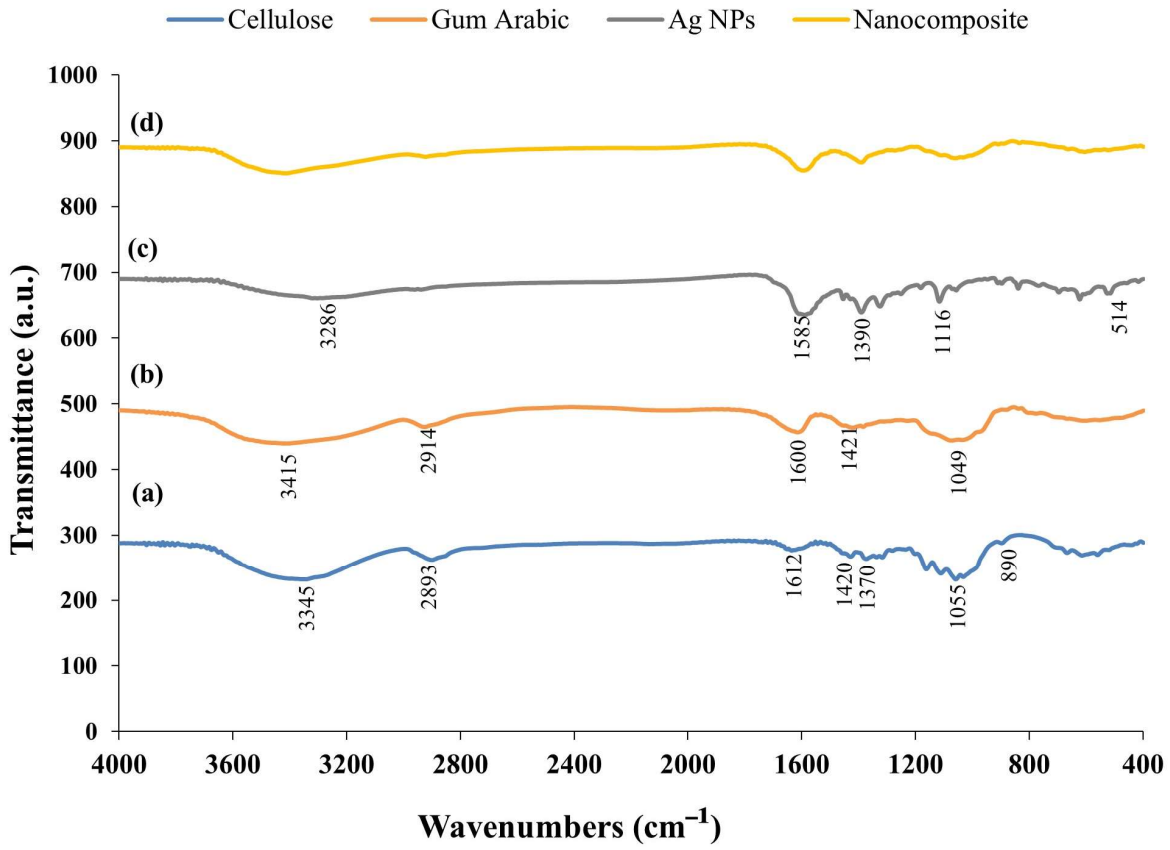

Figure 1. Fourier-transform infrared spectroscopy of (a) cellulose, (b) gum Arabic, (c) Ag nanoparticles, and (d) cellulose/gum Arabic/Ag nanocomposite.

The 1049 cm^{-1} peak in gum Arabic seems to be connected to C–OH extension vibration [27]. The existence of a significant quantity of hydroxyl and carboxyl groups and potential hydrogen bonding between them results in the widening of the peaks at 3400 and 1000 cm^{-1}. As the concentration of gum Arabic increases, a greater number of hydroxyl groups participate in bonding with hydrogen, resulting in further widening of the peak and a slight alteration in the C–O stretching frequency at 1049 cm^{-1} [28].

In the FTIR spectrum of silver nanoparticles, strong peaks at 1391 cm^{-1} correspond to elongation vibrations of the C–N bond. The spikes at 1116 cm^{-1} are a result of ether linkages and demonstrate the existence of substances absorbed on the exterior of silver metal nanoparticles. Additionally, the spikes at 1585 cm^{-1} are a result of the elongation of the C=C bond. The elongation vibrations of the O–H bond were detected at 3286 cm^{-1} [29]. The maximum corresponding to 514 cm^{-1} was due to the existence of Ag–O or pristine silver nanoparticles [30].

The FTIR spectrum of cellulose–gum Arabic–silver nanocomposite exhibited a blend of attributes from all components. The absorption band suggests the formation of a hydrogen bond between the hydroxyl group of the cellulose biopolymer and the silver nanoparticles. Furthermore, the alterations in wave numbers and the magnitude of other peaks demonstrate a robust association between the

cellulose biopolymer and the silver nanoparticles through hydrogen bonding, thus verifying the creation of a nanocomposite [31].

By comparing the spectra of the individual constituents with the FTIR spectrum of the final synthesized nanocomposite, one can logically infer that the spectrum of the ultimate nanocomposite is a result of the superposition of the spectra of its constituents, thus substantiating the optimal formation of the ultimate nanocomposite.

FTIR analysis revealed the formation of hydrogen bonds between the hydroxyl groups of cellulose and silver nanoparticles, indicating a strong interaction between the components. The absorption band at 3345 cm^{-1} corresponds to the O–H stretching vibration, while the peak at 1055 cm^{-1} is attributed to the C–O stretching vibration in cellulose. The presence of these peaks in the nanocomposite spectrum confirms the successful incorporation of silver nanoparticles into the cellulose–gum Arabic matrix.

3.2. XRD analysis

XRD analysis examined the arrangement of cellulose biopolymer samples (Figure 2a), gum Arabic (Figure 2b), silver nanoparticles (Figure 2c), and the cellulose–gum Arabic–silver nanocomposite (Figure 2d). The XRD pattern of cellulose exhibited peaks at approximately 15, 23, and 35°, corresponding to the (110), (200), and (004) planes, respectively [32,33]. Additionally, results revealed the existence of a somewhat shapeless and partially crystalline state for gum Arabic [21]. The XRD pattern of silver nanoparticles exhibited a cubic lattice structure with faces positioned at the center. The Miller indices of the (111), (200), (220), and (311) planes were observed at approximately 20, 39, 45, 65, and 78°, respectively [29].

The XRD spectrum derived from the nanocomposite indicated that the final structure is influenced by the arrangement of silver nanoparticles and polymers, thus confirming the formation of the nanocomposite. The X-ray diffraction pattern acquired from the synthesized nanocomposite revealed that the dispersion and distribution of nanoparticles within the polymer matrix resulted in the elimination or broadening of peaks, as well as a decrease in peak intensity and a peak leftward shift. This phenomenon can be primarily attributed to the presence of cellulose and gum Arabic polymers, along with the preferential alignment of silver nanoparticles in the nanocomposite structure [21].

XRD analysis confirmed the crystalline structure of the nanocomposite, with peaks corresponding to cellulose, gum Arabic, and silver nanoparticles. The peaks at 15, 23, and 35° are characteristic of cellulose, while the peaks at 20, 39, 45, 65, and 78° correspond to the cubic structure of silver nanoparticles. The broadening of peaks and a leftward shift in the XRD spectrum of the nanocomposite indicate the uniform dispersion of nanoparticles within the polymer matrix.

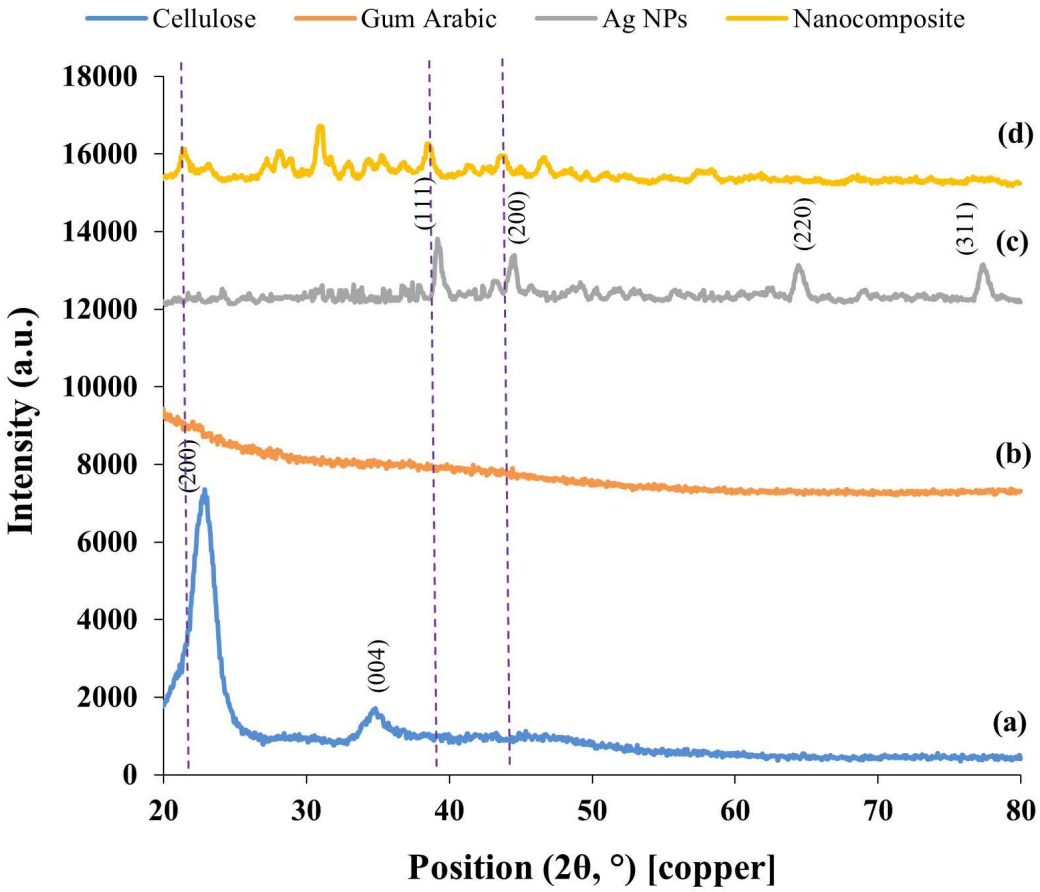

Figure 2. XRD pattern of (a) cellulose, (b) gum Arabic, (c) Ag nanoparticles, and (d) cellulose/gum Arabic/Ag nanocomposite.

3.3. SEM analysis

Scanning electron microscope pictures were employed to examine the arrangement and form of the produced cellulose–gum Arabic–silver nanocomposite (Figure 3). In the SEM picture produced from the nanocomposite, meshes with diverse holes formed by cellulose polymers and gum Arabic were detected. cellulose allocation information demonstrated that the generated bacterial cellulose samples had identical blending with equivalent dimensions. The configuration of the nanocomposite signifies that silver nanoparticles are situated in this polymer mesh.

The SEM image of the cellulose/GA/Ag nanocomposite revealed a mesh-like structure with uniform pores, indicating the successful integration of silver nanoparticles into the cellulose–gum Arabic matrix. The uniform distribution of silver nanoparticles within the polymer matrix was confirmed, which is crucial for ensuring consistent antimicrobial activity.

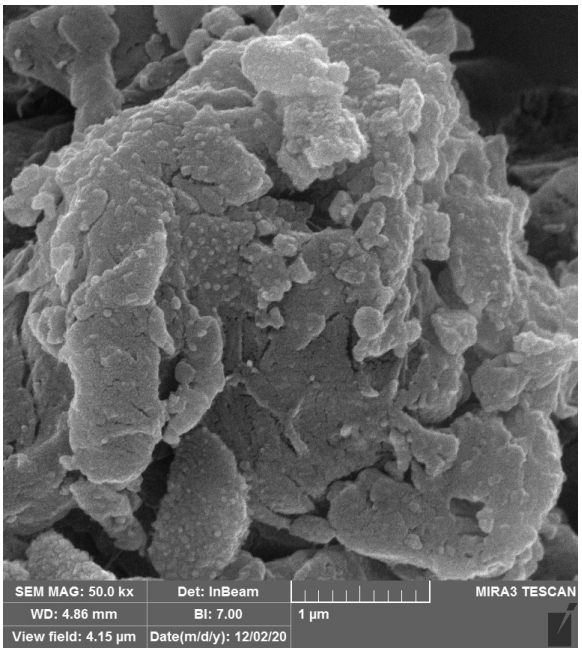

Figure 3. Scanning electron microscope image of cellulose/gum Arabic/Ag nanocomposite.

3.4. Energy-dispersive X-ray spectroscopy (EDS) and map analysis

EDS analysis (Figure 4) of the cellulose–gum Arabic–silver nanocomposite revealed the existence of component elements of the produced nanocomposite. These elements consist of silver (13.89% by weight), oxygen (24.33% by weight), calcium (0.38% weight), potassium (0.19% by weight), sodium (1.09% by weight), carbon (55.05% by weight), and nitrogen (5.07% by weight).

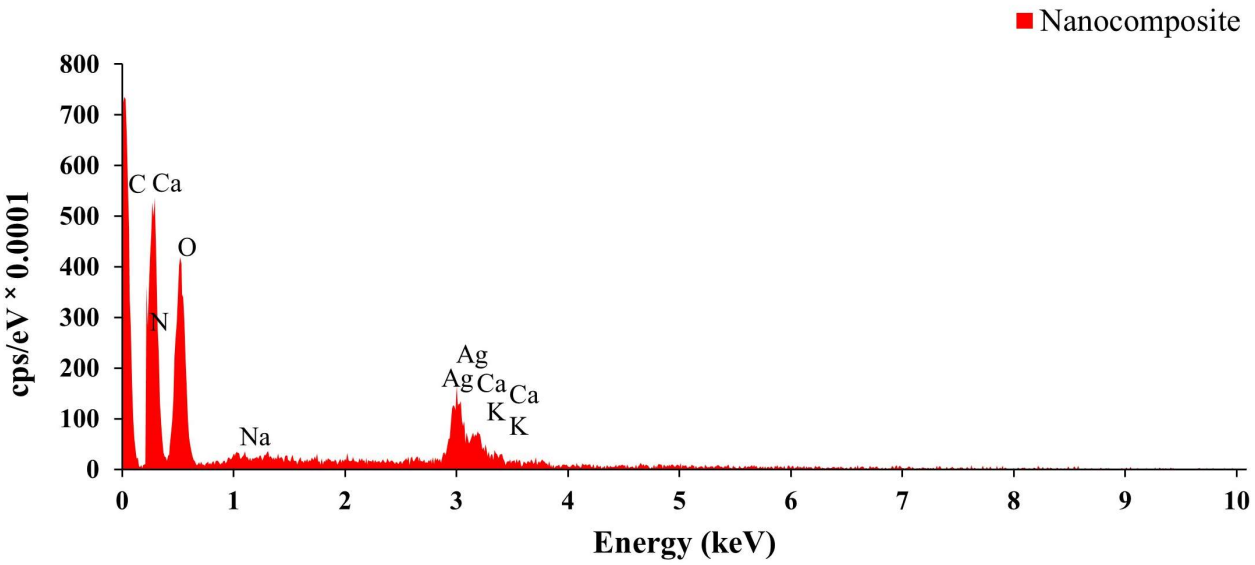

Figure 4. Energy dispersive X-ray pattern of cellulose/gum Arabic/Ag nanocomposite.

Figure 5 depicts the element arrangement on the exterior (map) of the cellulose–gum Arabic nanocomposite. The even dispersal of silver, O, Ca, K, Na, C, and N elements in the entire structure of the produced nanocomposite validated its creation.

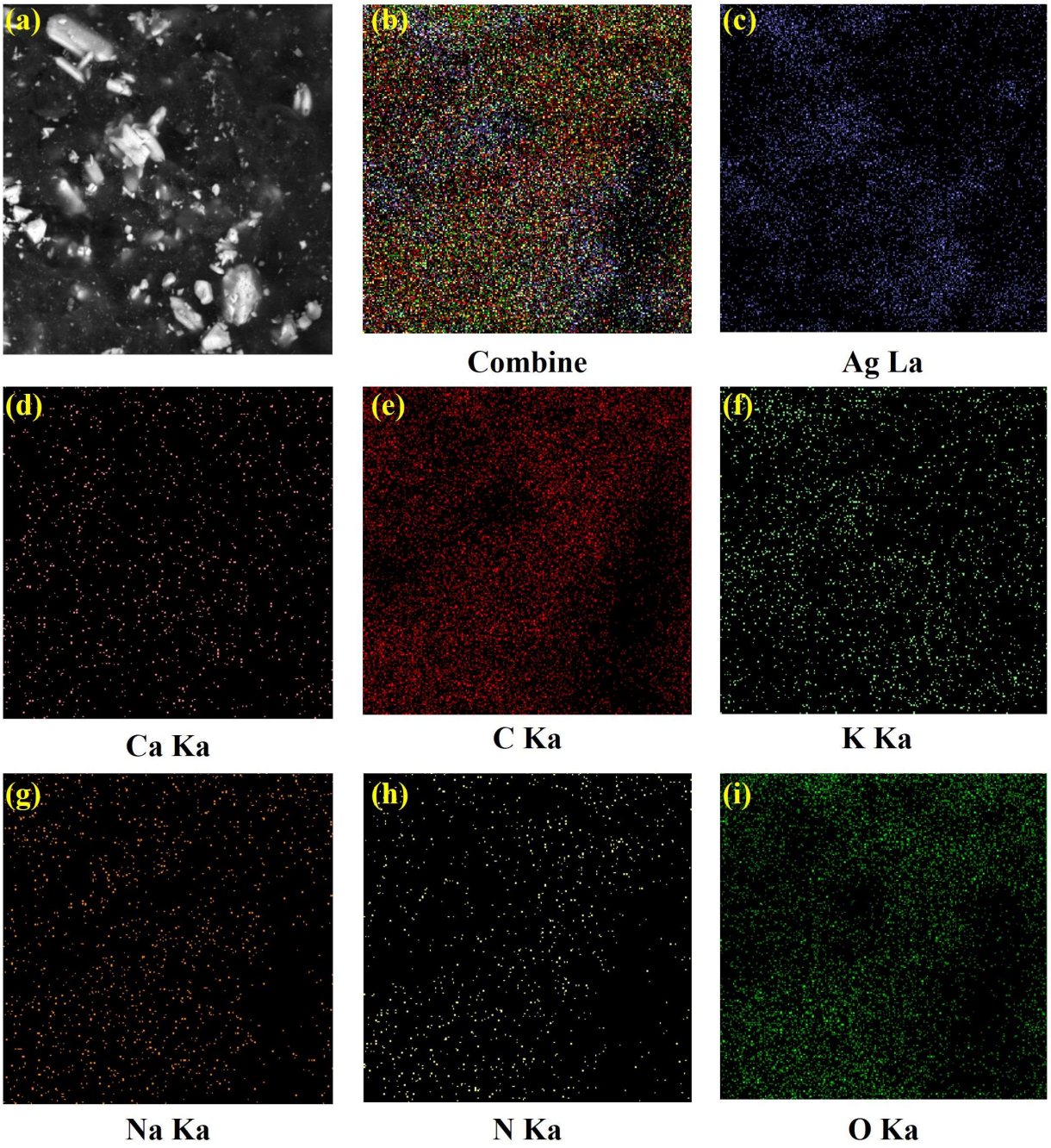

Figure 5. Dispersion map of composition components on the surface of (a) the final nanocomposite, (b) all elements, (c) silver, (d) calcium, (e) carbon, (f) potassium, (g) sodium, (h) nitrogen, and (i) oxygen.

3.5. TEM analysis

In order to investigate the morphology and dispersion of silver nanoparticles in the cellulose and gum Arabic biopolymer, a TEM micrograph was prepared from the cellulose–gum Arabic–silver nanocomposite (Figure 6). TEM micrograph evaluation showed the formation of the cellulose–gum Arabic–silver nanocomposite. Also, the morphology and length distribution of silver debris were investigated more precisely via transmission electron microscopy. The results confirmed that silver nanoparticles had optimally dispersed inside the biopolymeric cellulose and gum Arabic. The TEM photograph of the nanocomposite confirmed that the silver nanoparticles were uniformly located inside the field.

SEM and TEM images showed a uniform distribution of silver nanoparticles within the cellulose–gum Arabic matrix. The SEM image revealed a mesh-like structure with uniform pores, indicating the successful integration of silver nanoparticles. TEM analysis confirmed the optimal dispersion of silver nanoparticles, with an average particle size of 20–30 nm. A uniform distribution of nanoparticles is crucial for ensuring consistent antimicrobial activity.

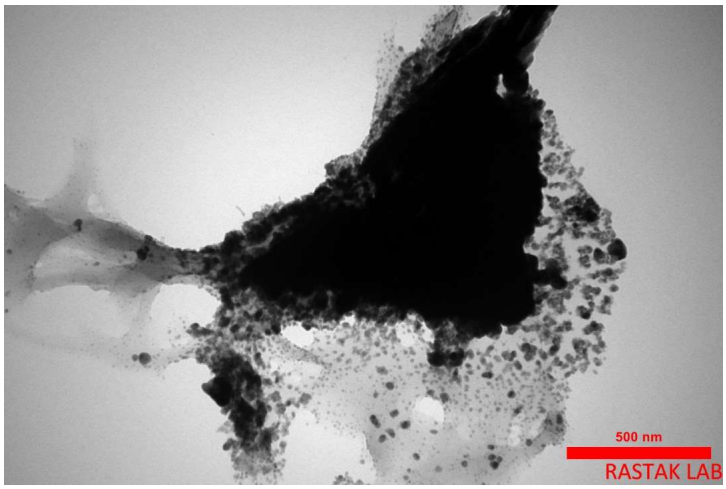

Figure 6. TEM image of cellulose/gum Arabic/Ag nanocomposite.

3.6. UV-vis analysis

Ultraviolet–visible spectroscopy was used to examine the optical absorption spectrum of cellulose, gum Arabic, silver nanoparticles, and the resulting nanocomposite. Figure 7 displays the spectrum in the 200–800 nm range. The peak wavelength at 270 nm indicates the existence of cellulose polymer (a). The lack of a distinct absorption peak in the diagram of gum Arabic polymer (b) suggests varying particle dimensions for this substance. Furthermore, a broad absorption peak was detected in the diagram of silver nanoparticles (c) within the approximate wavelength range of 420 nm. Moreover, the peak absorption for the produced nanocomposite (d) was detected at 423 nm, which is similar to the result achieved for the produced silver nanoparticles and verified the completion of the nanocomposite synthesis [21].

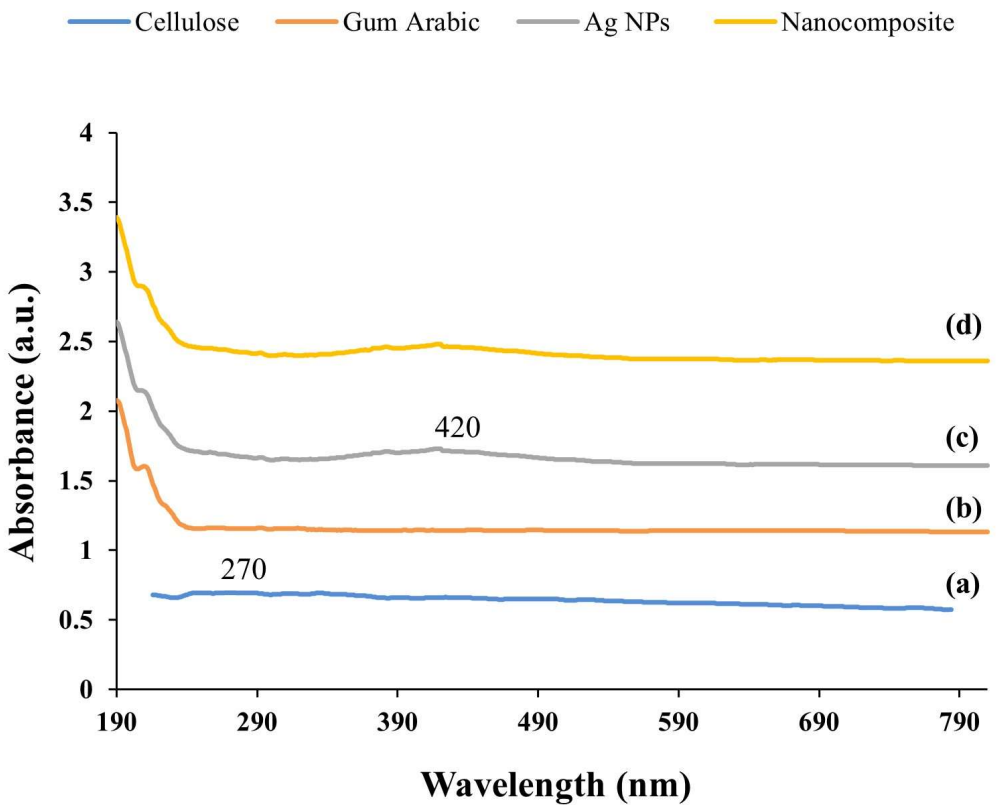

Figure 7. UV-vis analysis of (a) cellulose, (b) gum Arabic, (c) Ag nanoparticles, and (d) cellulose/gum Arabic/Ag nanocomposite.

3.7. TGA-DTA analysis

Thermal analysis was conducted from an ambient temperature of 800 °C with a heating rate of 20 °C/min in the presence of argon gas. Figure 8 demonstrates the thermal characteristics of cellulose (a) and the resultant nanocomposite (b), with each graph displaying significant decreases in weight. The initial phase occurred as a result of the dehydration process of the prepared samples. This interval for the cellulose polymer falls within the range of 20–200 °C, while for the synthesized nanocomposite, this falls within the range of 20–185 °C. Considering the drying circumstances, the elimination of moisture is connected to the comparative makeup of the samples, which was performed during this phase. The existence of various polymer constituents in the nanocomposite can enhance the quantity of soaked water. The subsequent phase of weight reduction took place for cellulose within the range of 200–390 °C; for the nanocomposite, it occurred within the range of 185–375 °C, which was connected to the disintegration of cellulose and gum Arabic linkages within the nanocomposite. The existence of silver nanoparticles in the nanocomposite enhanced its heat resistance, in contrast to the cellulose polymer in the subsequent phase. During the final phase of weight reduction, specifically at temperatures exceeding 400 °C, the connections between potential contaminants and the water structure linked as hydroxyl groups started to deteriorate and discharge [31].

TGA-DSC analysis demonstrated the thermal stability of the nanocomposite, with a significant weight loss at 375 °C, corresponding to the degradation of cellulose and gum Arabic. The presence of silver nanoparticles enhanced the thermal stability of the nanocomposite, as evidenced by the higher

degradation temperature compared to pure cellulose. This improved thermal stability is essential for the long-term performance of the nanocomposite in biomedical applications.

TGA and DSC were conducted to evaluate the thermal stability of the raw materials and the synthesized cellulose/GA/Ag nanocomposite. Figure 8 shows the TGA curves of the raw materials: bacterial cellulose, gum Arabic, and silver nanoparticles. Bacterial cellulose exhibited a significant weight loss at 200–390 °C, corresponding to the degradation of cellulose fibers. gum Arabic showed a weight loss at 185–375 °C, attributed to the decomposition of polysaccharide chains. Silver nanoparticles exhibited high thermal stability, with minimal weight loss over the temperature range.

The DSC analysis revealed an endothermic peak at 375 °C, further confirming the thermal stability of the nanocomposite. The comparison between the raw materials and the nanocomposite highlights the improved thermal stability resulting from the modification process, confirming the successful formation of the bionanocomposite.

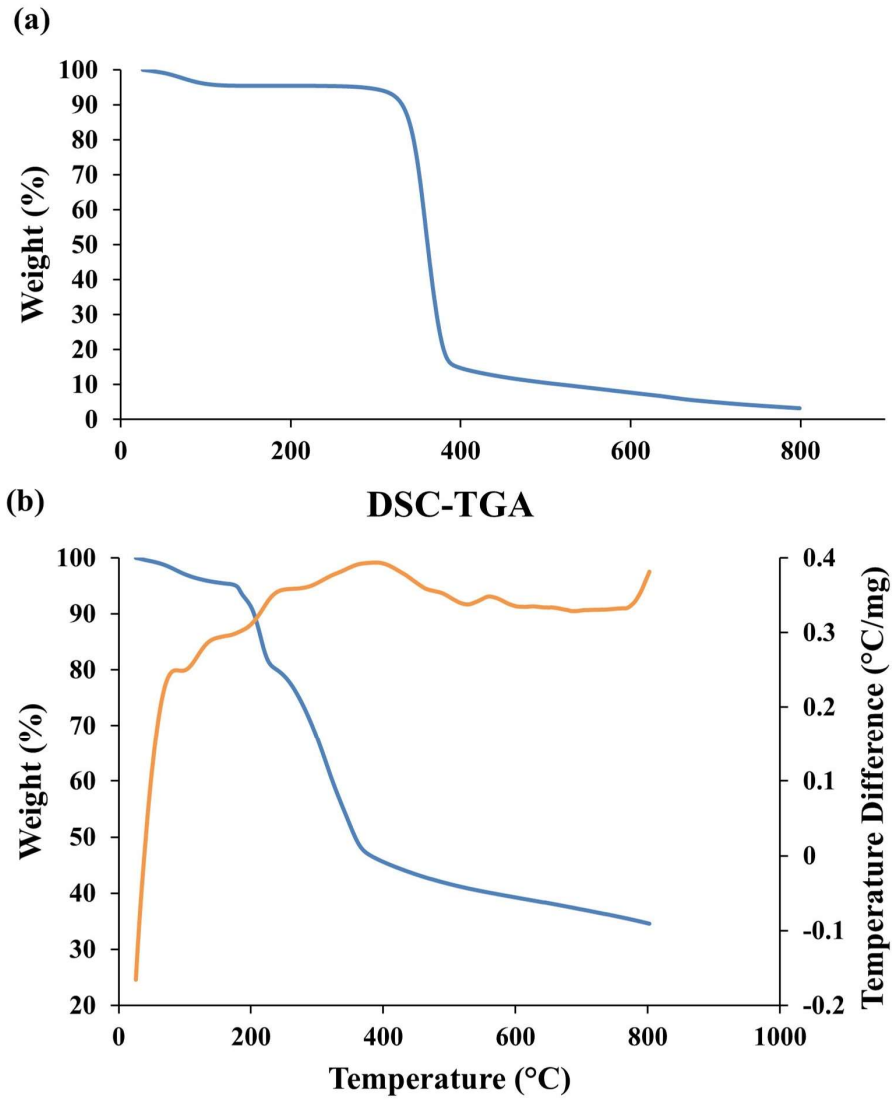

Figure 8. Thermogravimetric analysis (TGA) of (a) cellulose and (b) TGA-DTA of cellulose/gum Arabic/Ag nanocomposite.

3.8. Antibacterial activity

To evaluate the most favorable circumstances for the creation of the cellulose–gum Arabic–silver nanocomposite exhibiting the greatest antibacterial potential, nine trials were formulated utilizing the Taguchi approach. The outcomes of the different nanocomposites on the vitality of *S. mutans* microorganisms are shown in Figure 9.

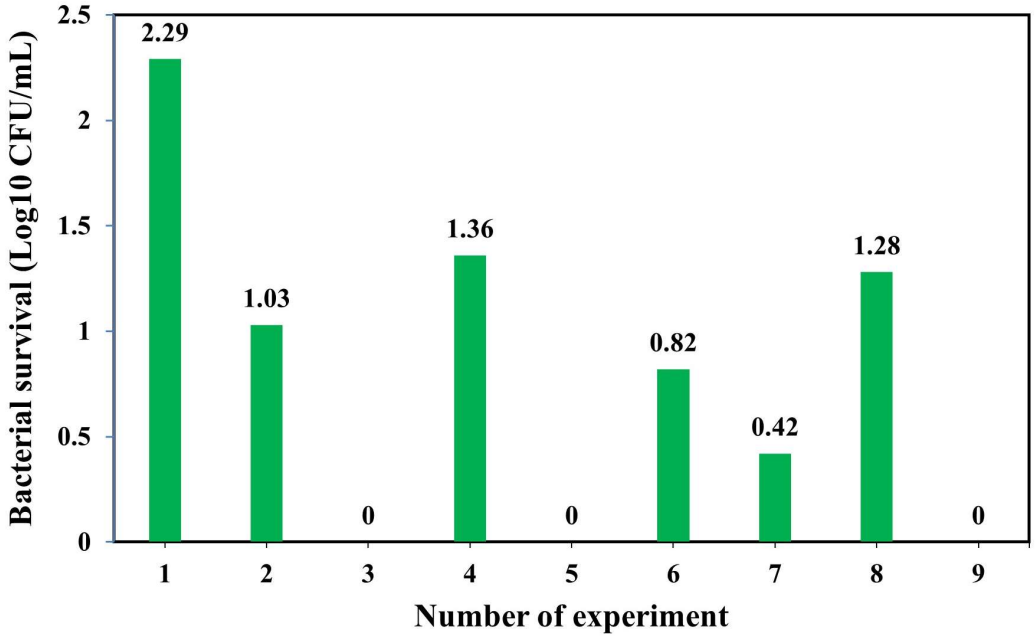

Figure 9. Effects of nanocomposites synthesized under different conditions on the survival rate of *Streptococcus mutans* bacteria.

Results show that the nanocomposites produced under test condition 3 (2 mg/mL of cellulose, 3 mg/mL of gum Arabic, and 6 mg/mL of silver), test condition 5 (4 mg/mL of cellulose, 2 mg/mL of gum Arabic, and 6 mg/mL of silver), and test condition 9 (6 mg/mL of cellulose, 3 mg/mL of gum Arabic, and 4 mg/mL of silver) exhibited the most potent antibacterial effect against *S. mutans* biofilm. Furthermore, the presence of the nanocomposite resulted in a survival rate of the bacteria that dropped to its minimum level, i.e., zero. The antibacterial effect of silver nanoparticles depends on proteoglycans present within the bacterial membrane, which serve as attachment points for both silver nanoparticles and ions. In addition, silver ions can interact with sulfuryl groups during protein synthesis and thus interfere with bacterial DNA replication [34]. As a result, nanocomposites that include these nanoparticles can serve the same purpose through a comparable mechanism. Figure 10 illustrates how the viability of *S. mutans* bacteria is influenced by cellulose, gum Arabic, and silver nanoparticles. Results indicate that at the third level, the vitality of *S. mutans* was predominantly impacted by cellulose, gum Arabic, and silver components.

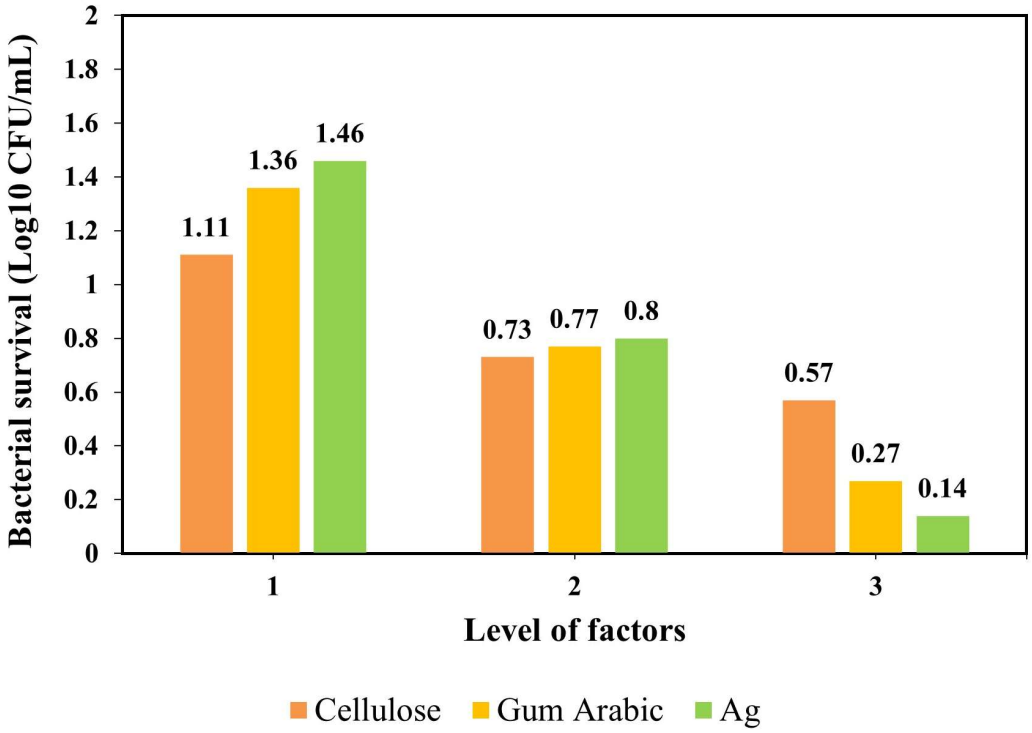

Figure 10. Effect of cellulose, gum Arabic, and Ag nanoparticles (separately) on the survival rate of *Streptococcus mutans*.

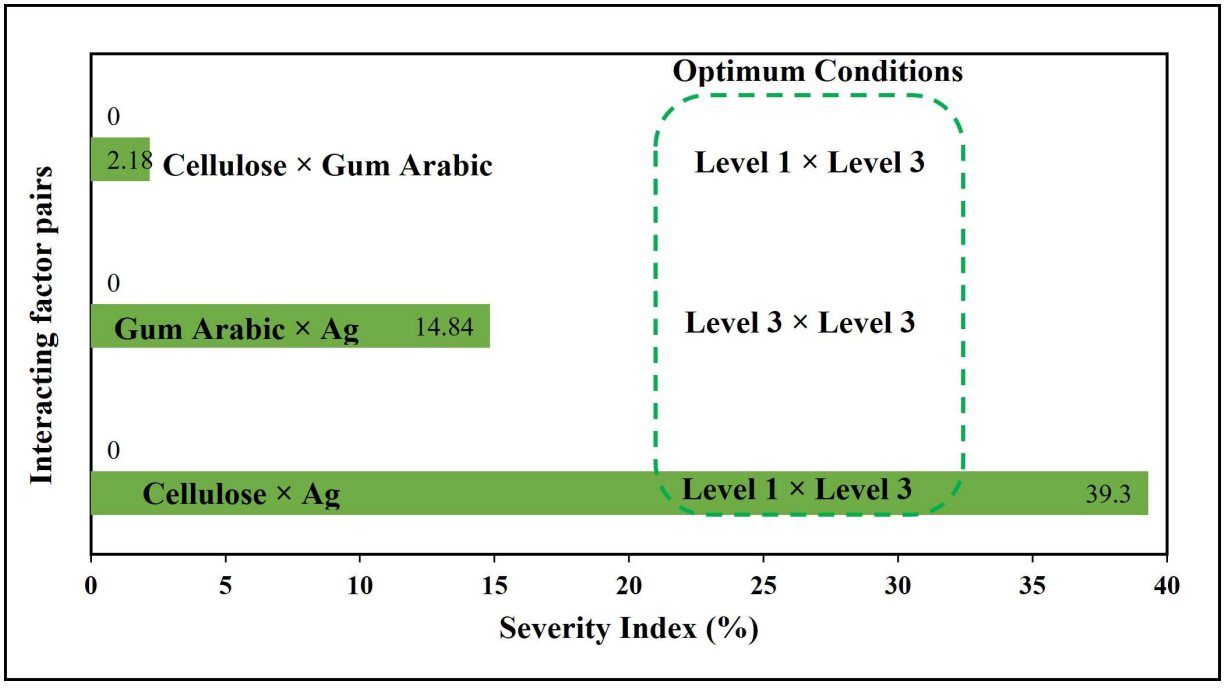

Figure 11. Effect of interactions between the studied factors on growth inhibition of *Streptococcus mutans*.

The interdependence of variables on the viability of *S. mutans* is illustrated in Figure 11. At the primary tier, cellulose and silver exhibited the highest degree of interdependence, impacting each other

and the viability of *S. mutans* by 39.30%. The synergistic impact of gum Arabic and silver yielded a unique interaction effect on the viability of *S. mutans*, which was observed at the third tier, corresponding to a value of 14.84%. The minimal magnitude of the degree of mutual influence intensity index was found to be linked to cellulose at the initial stage and gum Arabic at the third level, at a rate of 2.18%.

Table 2 shows the variance analysis of parameters affecting the survival rate of *S. mutans*. After examining the data, it was determined that silver had the most substantial influence on the survivability of *S. mutans* bacteria, with an impact of 53.22%. Following closely behind was gum Arabic, with an effect of 35.55%, while cellulose had a milder effect of 8.86%.

Table 2. Analysis of variance of factors affecting the survival rate of *Streptococcus mutans*.

Factors	DOF	Sum of squares	Variance	F ratio (F)	Pure sum	Percent (%)
Cellulose	2	0.46	0.23	15.99	0.43	8.86
Gum Arabic	2	1.76	0.88	61.12	1.74	35.55
Ag	2	2.63	1.31	91.00	2.60	53.22

DOF: Degree of freedom.

The optimal conditions for producing a cellulose–gum Arabic–silver nanocomposite with the greatest antibacterial activity were estimated by analyzing each factor and their interplay (as shown in Table 3). Based on the findings, the bacterial viability of *S. mutans* was most affected by the presence of silver, whereas cellulose had the least impact. gum Arabic, on the other hand, demonstrated an intermediate effect similar to that of silver. The third tier was identified as the optimal tier for all three components. The results indicate that under favorable circumstances, the nanocomposite prevented bacterial activity by –0.62. This value was the nearest, and superior, to the outcomes of experiments 3, 5, and 9.

Table 3. Optimum conditions for the synthesis of cellulose/gum Arabic/Ag nanocomposites with the highest antibacterial activity.

Factors	Level	Contribution
Cellulose	3	0.23
GA	3	0.53
Ag	3	0.66
Total contribution from all factors		1.42
Current grand average of performance		0.80
Bacterial survival at optimum condition		–0.62

The antibacterial activity of the cellulose/GA/Ag bionanocomposite was evaluated against *S. mutans*, a key pathogen in dental caries. The results demonstrated that the nanocomposite synthesized under optimal conditions (2 mg/mL cellulose, 3 mg/mL gum Arabic, and 6 mg/mL silver nanoparticles) achieved a 100% reduction in bacterial viability, with a bacterial survival rate of 0 Log10 CFU/mL. This section provides an in-depth analysis of the factors contributing to the antibacterial efficacy of the nanocomposite.

Silver nanoparticles are well-known for their broad-spectrum antimicrobial activity. The primary mechanism involves the release of silver ions (Ag^+), which interact with bacterial cell membranes and intracellular components, leading to cell death. Silver ions can bind to thiol groups (–SH) in bacterial proteins, disrupting enzymatic activity and cellular respiration. Additionally, silver ions can interact with bacterial DNA, inhibiting replication and transcription processes. The small size and high surface area of silver nanoparticles enhance their antimicrobial efficacy by facilitating the penetration of bacterial cell walls and membranes.

Bacterial cellulose and gum Arabic play crucial roles in enhancing the stability and dispersion of silver nanoparticles within the nanocomposite, thereby improving their antimicrobial efficacy. At the same time, neither bacterial cellulose nor gum Arabic exhibit inherent antimicrobial activity; their combination with silver nanoparticles creates a synergistic effect that enhances the overall performance of the nanocomposite. Bacterial cellulose, with its nanofiber structure and high surface area, provides a robust matrix for the uniform distribution of silver nanoparticles. This ensures the sustained release of silver ions, prolonging the antimicrobial effect. gum Arabic, a natural polysaccharide, forms stable complexes with silver nanoparticles, preventing their aggregation and enhancing their bioavailability. The combination of these biopolymers not only improves the mechanical and thermal properties of the nanocomposite but also enhances its antimicrobial efficacy.

Bacterial cellulose, with its nanofiber structure and high surface area, provides a robust matrix for the uniform distribution of silver nanoparticles. This ensures the sustained release of silver ions, prolonging the antimicrobial effect. The nanofiber network of bacterial cellulose also acts as a physical barrier, preventing the aggregation of silver nanoparticles and maintaining their high surface area, which is crucial for maximizing their antimicrobial activity.

Gum Arabic, a natural polysaccharide, forms stable complexes with silver nanoparticles, preventing their aggregation and enhancing their bioavailability. The presence of hydroxyl and carboxyl groups in gum Arabic facilitates the formation of hydrogen bonds with silver nanoparticles, ensuring their uniform dispersion within the nanocomposite. This uniform dispersion is essential for achieving consistent and effective antimicrobial activity.

The combination of bacterial cellulose and gum Arabic creates a synergistic effect that enhances the antimicrobial efficacy of silver nanoparticles. Bacterial cellulose provides a stable matrix for the uniform distribution of silver nanoparticles, while gum Arabic prevents their aggregation and enhances their bioavailability. This synergistic effect ensures sustained release of silver ions, leading to prolonged antimicrobial activity and improved performance against *Streptococcus mutans*.

The choice of bacterial cellulose and gum Arabic was based on their unique properties and cost-effectiveness. Bacterial cellulose is a natural biomaterial with exceptional physicochemical properties, including high mechanical strength, biocompatibility, and water retention capacity. Gum Arabic is a natural polysaccharide with excellent emulsifying, stabilizing, and biocompatible properties. Both materials are cost-effective and sustainable, making them ideal candidates for use in biomedical applications. The combination of these biopolymers with silver nanoparticles not only enhances the antimicrobial efficacy of the nanocomposite but also improves its mechanical and thermal properties, making it a promising candidate for various medical and dental applications.

The antibacterial activity of the cellulose/GA/Ag nanocomposite can be attributed to the synergistic effects of its components: bacterial cellulose, gum Arabic, and silver nanoparticles. The characterization results support the proposed antimicrobial mechanism. FTIR analysis revealed the formation of hydrogen bonds between the hydroxyl groups of cellulose and silver nanoparticles,

indicating a strong interaction between the components. XRD analysis confirmed the crystalline structure of the nanocomposite, with peaks corresponding to cellulose, gum Arabic, and silver nanoparticles. SEM and TEM images showed a uniform distribution of silver nanoparticles within the cellulose-gum Arabic matrix, further supporting the enhanced dispersion and stability of the nanoparticles. TGA-DSC analysis demonstrated the thermal stability of the nanocomposite, with a significant weight loss at 375 °C, corresponding to the degradation of cellulose and gum Arabic.

This study builds on previous research by addressing several key limitations. While previous studies have explored the use of cellulose-based nanocomposites for antimicrobial applications, many have focused on single-component systems or lacked systematic optimization of synthesis conditions. The findings of this study are consistent with recent research on cellulose-based nanocomposites and antimicrobial materials. For instance, Sathiyaseelan et al. (2024) demonstrated the use of cellulose-based nanocomposites for the inhibition of bacterial pathogens and food safety applications, highlighting their high antimicrobial activity and stability. Their study emphasized the importance of optimizing the synthesis conditions to achieve maximum antimicrobial efficacy, which aligns with our use of the Taguchi method to optimize the levels of cellulose, gum Arabic, and silver nanoparticles [35].

Similarly, Mariadoss et al. (2023) explored the use of cellulose-based materials as an effective antibacterial agent, focusing on their antimicrobial properties. Their findings support our results, demonstrating that the combination of cellulose with other biopolymers and nanoparticles can significantly enhance the antimicrobial efficacy of the resulting nanocomposite. These studies underscore the potential of cellulose-based nanocomposites as effective antimicrobial agents in various applications [36].

The cellulose/GA/Ag nanocomposite developed in this study has significant potential for medical and dental applications. Its high antimicrobial efficacy, biocompatibility, and cost-effectiveness make it a promising candidate for use in wound dressings, dental fillings, and antimicrobial coatings. The sustained release of silver ions from the nanocomposite ensures long-term antimicrobial activity, reducing the risk of bacterial resistance. Furthermore, the use of natural biopolymers such as bacterial cellulose and gum Arabic enhances the sustainability and environmental friendliness of the material.

4. Conclusions

The findings of the current investigation demonstrated that the cellulose–gum Arabic–silver nanocomposite, produced through the process of direct blending, exhibits advantageous antimicrobial characteristics in combating *S. mutans*. Nanocomposite produced in ideal circumstances (silver with an efficacy of 53.22%, gum Arabic with an efficacy of 35.55%, and cellulose with an efficacy of 8.86%) had a negative effect on bacterial proliferation, inhibiting bacterial activity and completely halting its growth and viability. The release of silver ions, combined with the stabilizing effects of bacterial cellulose and gum Arabic, results in a highly effective antimicrobial material. The characterization results confirm the successful formation and stability of the nanocomposite, supporting its potential for various biomedical applications. Future studies should focus on evaluating the long-term stability and biocompatibility of the nanocomposite in vivo, as well as exploring its potential in other antimicrobial applications. Therefore, this particular nanocomposite possesses the potential to function as a potent agent against microbial organisms and biofilms in various medical and dental fields.

Use of AI tools declaration

The authors declare they have not used Artificial Intelligence (AI) tools in the creation of this article.

Acknowledgments

This work was supported by grants (990292) from the Kermanshah University of Medical Sciences.

Author contributions

Mohsen Safaei was responsible for conceptualization, methodology, resources, project administration, funding acquisition, and supervision; Bahram Azizi and Ehsan Shoohanizad were responsible for investigation; Mohammad Salmani Mobarakeh was responsible for data analysis, writing, advisor, and visualization; Ling Shing Wong was responsible for supervision, methodology, investigation, and resources; Nafiseh Nikkerdar was responsible for investigation.

Conflict of interest

The authors declare no competing interests.

Data availability

The data used to support the findings of this study are included in the article.

References

1. Pourhajibagher M, Bahador A (2021) Synergistic biocidal effects of metal oxide nanoparticles-assisted ultrasound irradiation: Antimicrobial sonodynamic therapy against *Streptococcus mutans* biofilms. *Photodiagnosis Photodyn Ther* 35: 102432. https://doi.org/10.1016/j.pdpdt.2021.102432
2. Sharifi R, Vatani A, Sabzi A, et al. (2024) A narrative review on application of metal and metal oxide nanoparticles in endodontics. *Heliyon* 10: e34673. https://doi.org/10.1016/j.heliyon.2024.e34673
3. Rostami-Vartooni A, Moradi-Saadatmand A (2019) Green synthesis of magnetically recoverable Fe_3O_4/HZSM-5 and its Ag nanocomposite using *Juglans regia* L. leaf extract and their evaluation as catalysts for reduction of organic pollutants. *IET Nanobiotechnol* 13: 407–415. https://doi.org/10.1049/iet-nbt.2018.5089
4. Moradpoor H, Safaei M, Golshah A, et al. (2021) Green synthesis and antifungal effect of titanium dioxide nanoparticles on oral *Candida albicans* pathogen. *Inorg Chem Commun* 130: 108748. https://doi.org/10.1016/j.inoche.2021.108748
5. Khodadadi B, Bordbar M, Yeganeh-Faal A, et al. (2017) Green synthesis of Ag nanoparticles/clinoptilolite using *Vaccinium macrocarpon* fruit extract and its excellent catalytic activity for reduction of organic dyes. *J Alloys Compd* 719: 82–88. https://doi.org/10.1016/j.jallcom.2017.05.135

6. Demirkan B, Bozkurt S, Şavk A, et al. (2019) Composites of bimetallic platinum-cobalt alloy nanoparticles and reduced graphene oxide for electrochemical determination of ascorbic acid, dopamine, and uric acid. *Sci Rep* 9: 12258. https://doi.org/10.1038/s41598-019-48802-0
7. Mohammadi H, Moradpoor H, Beddu S, et al. (2025) Current trends and research advances on the application of TiO_2 nanoparticles in dentistry: How far are we from clinical translation? *Heliyon* 11: e42169. https://doi.org/10.1016/j.heliyon.2025.e42169
8. Aygün A, Gülbağça F, Nas MS, et al. (2019) Biological synthesis of silver nanoparticles using *Rheum ribes* and evaluation of their anticarcinogenic and antimicrobial potential: A novel approach in phytonanotechnology. *J Pharm Biomed Anal* 179: 113012. https://doi.org/10.1016/j.jpba.2019.113012
9. De Jesús Ruíz-Baltazar Á, Reyes-López SY, De Lourdes Mondragón-Sánchez M, et al. (2018) Biosynthesis of Ag nanoparticles using *Cynara cardunculus* leaf extract: Evaluation of their antibacterial and electrochemical activity. *Results Phys* 11: 1142–1149. https://doi.org/10.1016/j.rinp.2018.11.032
10. Mourdikoudis S, Kostopoulou A, LaGrow AP (2021) Magnetic nanoparticle composites: Synergistic effects and applications. *Adv Sci* 8: 2004951. https://doi.org/10.1002/advs.202004951
11. Lim JYC, Goh L, Otake KI, et al. (2023) Biomedically-relevant metal organic framework-hydrogel composites. *Biomater Sci* 11: 2661–2677. https://doi.org/10.1039/D2BM01906J
12. Safaei M, Taran M (2021) Preparation of bacterial cellulose fungicide nanocomposite incorporated with MgO nanoparticles. *J Polym Environ* 30: 2066–2076. https://doi.org/10.1007/s10924-021-02329-6
13. Zhong C (2020) Industrial-scale production and applications of bacterial cellulose. *Front Bioeng Biotechnol* 8: 605374. https://doi.org/10.3389/fbioe.2020.605374
14. Sethuraman S, Rajendran K (2018) Multicharacteristic behavior of tyrosine present in the microdomains of the macromolecule gum arabic at various pH conditions. *ACS Omega* 3: 17602–17609. https://doi.org/10.1021/acsomega.8b02928
15. Dang X, Fu Y, Wang X (2024) Versatile biomass-based injectable photothermal hydrogel for integrated regenerative wound healing and skin bioelectronics. *Adv Funct Mater* 34: 2405745. https://doi.org/10.1002/adfm.202405745
16. Dang X, Yu Z, Wang X, et al. (2023) Eco-friendly cellulose-based nonionic antimicrobial polymers with excellent biocompatibility, nonleachability, and polymer miscibility. *ACS Appl Mater Interfaces* 15: 50344–50359. https://doi.org/10.1021/acsami.3c10902
17. Dang X, Yu Z, Wang X, et al. (2023) Sustainable one-pot synthesis of novel soluble cellulose-based nonionic biopolymers for natural antimicrobial materials. *Chem Eng J* 468: 143810. https://doi.org/10.1016/j.cej.2023.143810
18. Yin H, Liu F, Abdiryim T, et al. (2024) Sodium carboxymethyl cellulose and MXene reinforced multifunctional conductive hydrogels for multimodal sensors and flexible supercapacitors. *Carbohydr Polym* 327: 121677. https://doi.org/10.1016/j.carbpol.2023.121677
19. Raiszadeh-Jahromi Y, Rezazadeh-Bari M, Almasi H, et al. (2020) Optimization of bacterial cellulose production by *Komagataeibacter xylinus* PTCC 1734 in a low-cost medium using optimal combined design. *J Food Sci Technol* 57: 2524–2533. https://doi.org/10.1007/s13197-020-04289-6

20. Dasaradhudu Y, Srinivasan MA (2020) Synthesis and characterization of silver nanoparticles using co-precipitation method. *Mater Today Proc* 33: 720–723. https://doi.org/10.1016/j.matpr.2020.06.029
21. Safaei M, Taran M (2017) Fabrication, characterization, and antifungal activity of sodium hyaluronate-TiO_2 bionanocomposite against *Aspergillus niger*. *Mater Lett* 207: 113–116. https://doi.org/10.1016/j.matlet.2017.07.038
22. Zhang G, Lu M, Liu R, et al. (2020) Inhibition of *Streptococcus mutans* biofilm formation and virulence by *Lactobacillus plantarum* K41 isolated from traditional Sichuan pickles. *Front Microbiol* 11: 774. https://doi.org/10.3389/fmicb.2020.00774
23. Safaei M, Moghadam A (2022) Optimization of the synthesis of novel alginate-manganese oxide bionanocomposite by Taguchi design as antimicrobial dental impression material. *Mater Today Commun* 31: 103698. https://doi.org/10.1016/j.mtcomm.2022.103698
24. Ottah VE, Ezugwu AL, Ezike TC, et al. (2022) Comparative analysis of alkaline-extracted hemicelluloses from Beech, African rose and Agba woods using FTIR and HPLC. *Heliyon* 8: e09714. https://doi.org/10.1016/j.heliyon.2022.e09714
25. Soni B, Hassan EB, Mahmoud B (2015) Chemical isolation and characterization of different cellulose nanofibers from cotton stalks. *Carbohydr Polym* 134: 581–589. https://doi.org/10.1016/j.carbpol.2015.08.031
26. Safaei M, Mobarakeh MS, Azizi B, et al. (2024) Chitosan/Arabic gum/ZnO bionanocomposite as a novel antibacterial agent. *Polimery* 69: 362–370. https://doi.org/10.14314/polimery.2024.6.4
27. Venkatesan J, Hur W, Gupta PK, et al. (2023) Gum Arabic-mediated liquid exfoliation of transition metal dichalcogenides as photothermic anti-breast cancer candidates. *Int J Biol Macromol* 244: 124982. https://doi.org/10.1016/j.ijbiomac.2023.124982
28. Wang J, Yang H, Luo L, et al. (2024) Persimmon leaf polyphenols as potential ingredients for modulating starch digestibility: Effect of starch-polyphenol interaction. *Int J Biol Macromol* 270: 132524. https://doi.org/10.1016/j.ijbiomac.2024.132524
29. Anandalakshmi K, Venugobal J, Ramasamy V (2015) Characterization of silver nanoparticles by green synthesis method using *Pedalium murex* leaf extract and their antibacterial activity. *Appl Nanosci* 6: 399–408. https://doi.org/10.1007/s13204-015-0449-z
30. Hamouda RA, Alharthi MA, Alotaibi AS, et al. (2023) Biogenic nanoparticles silver and copper and their composites derived from marine alga *Ulva lactuca*: Insight into the characterizations, antibacterial activity, and anti-biofilm formation. *Molecules* 28: 6324. https://doi.org/10.3390/molecules28176324
31. Safaei M, Taran M, Imani MM, et al. (2019) Application of Taguchi method in the optimization of synthesis of cellulose-MgO bionanocomposite as antibacterial agent. *Pol J Chem Technol* 21: 116–122. https://doi.org/10.2478/pjct-2019-0047
32. Pang J, Mehandzhiyski AY, Zozoulenko I (2023) A computational study of cellulose regeneration: Coarse-grained molecular dynamics simulations. *Carbohydr Polym* 313: 120853. https://doi.org/10.1016/j.carbpol.2023.120853
33. Ye D, Rongpipi S, Kiemle SN, et al. (2020) Preferred crystallographic orientation of cellulose in plant primary cell walls. *Nat Commun* 11: 5720. https://doi.org/10.1038/s41467-020-18449-x
34. Padovani GC, Feitosa VP, Sauro S, et al. (2015) Advances in dental materials through nanotechnology: Facts, perspectives and toxicological aspects. *Trends Biotechnol* 33: 621–636. https://doi.org/10.1016/j.tibtech.2015.09.005

35. Sathiyaseelan A, Lu Y, Ryu S, et al. (2024) Synthesis of cytocompatible gum Arabic-encapsulated silver nitroprusside nanocomposites for inhibition of bacterial pathogens and food safety applications. *Environ Res* 263: 120246. https://doi.org/10.1016/j.envres.2024.120246
36. Mariadoss AVA, Saravanakumar K, Sathiyaseelan A, et al. (2023) Cellulose-graphene oxide nanocomposites encapsulated with green synthesized silver nanoparticles as an effective antibacterial agent. *Mater Today Commun* 35: 105652. https://doi.org/10.1016/j.mtcomm.2023.105652

AIMS Press